

# A Novel Method for Multi-Feature Grading of Mango Using Machine Vision



Jing Sun\*, Shuoming Li, Xin Yao

Department of Information Engineering, Zhongshan Polytechnic College, Zhongshan, China  
sunjing\_zspt@sina.com, lishuoming@whu.edu.cn, gotoyaoxin@163.com

Received 12 August 2019; Revised 3 January 2020; Accepted 2 March 2020

**Abstract.** The automatic quality inspection and grading application of mangoes, a widely cultivated fruit, is of paramount importance in post-harvest processing. Fruit features such as size, surface defects, and color are extracted using machine vision algorithms. A novel curve-fitting route algorithm CFR is proposed to improve the size measurement in image preprocessing. Surface defects are inspected and computed by utilizing image binarization techniques. Mango ripeness is analyzed and calibrated by utilizing the RGB color model. Finally, the Random Forests Classification technique is adopted in the machine learning layer to resolve the limitations in traditional multi-feature grading algorithms. Experimental results show that the accuracy of size calculation is nearly 98.4%, and the accuracy of quality grading received is up to 94.4%. Therefore, the proposed multi-feature grading method of mango (MFG) proved to be efficient and reliable.

**Keywords:** feature extraction, machine vision, multi-feature grading, Random Forests Classification

## 1 Introduction

Mango is a tropical fruit with great commercial prospects. In recent years, with growing plantation areas and increasing output, mango has become one of the five most widely planted fruits in the world. Asia is the largest mango-producing continent and accounts for approximately 76% of global mango production [1].

In many mango planting areas, the level of automation and efficiency of post-harvest processing is far from satisfactory in terms of accuracy and throughput: Although mango is a highly perishable fruit with a short shelf life, its post-harvest processing is still carried out manually through visual inspection [2]. If the mangoes are not processed in time after harvest, it may cost heavily to the mango planters.

For marketing purposes, mangoes are generally graded based on their external quality features: size, shape, ripeness and the presence and type of surface defects [3]. Because of its practicability and generality, the machine vision techniques are the most adopted options in recent system design, especially for applications in quality inspection and gradation. A machine vision system that can simulate the human grading process may classify mangoes into standardized groups based on their important characteristics as well it may greatly accelerate this process. To this end, in-depth studies are being conducted to design effective and reliable systems that can rapidly grade this particular variety of fruit. The accuracy and applicability of such systems are being explored.

### 1.1 Related Works

The research problems of a machine-vision based fruit grading systems vary from fruit to fruit. Therefore, most of the previous research works were focused on building dedicated systems for sorting a single variety of fruit. The machine vision based systems have been used in some inspection applications for

---

\* Corresponding Author

fruits such as mangoes [2-4], dates [5], tomatoes [6-8], kiwifruits [9] and blueberries [10]. In general, the performances of these works depend on the extracted features that are quantized and used in their design.

Momin et al. presented a speed grading method which classify mangoes into three classes by extracting only two fruit features: size and shape [2]. Region-based global thresholding, color binarization, and morphological analysis were applied in image processing. It was mentioned that the method had limitations in practical applications and a formal feature distribution based classification could improve fruit grading accuracy [2].

The inter-relationship between the fruit features extracted for grading is also important. The more the colors, textural, and morphological features considered in the grading process, the higher the grading accuracy. Nandi et al. developed a model of a mango fruit grading system [3]. In their system, several features that were sensitive to the maturity, size and surface deflection were extracted. To predict maturity, a Support Vector Machine (SVM) based classifier had been built. Finally, to solve the multi-feature classification problems, Multi Attribute Decision Making (MADM) theory was employed in their design. The grading accuracy received was less than 90% if human expert grading was assumed to be 100% accurate [3].

Sapan et al. used the Fuzzy inference system for the decision-making process to address the grading problems of mango production based on its maturity and size [4]. The time needed to grade a mango was 2.3 seconds and accuracy received was 89%. The limitations of their systems were: all mangoes must store at the same temperature; the time taken for grading of one single fruit was more than 2 seconds [4].

In recent proposals, deep convolutional neural networks (CNN) feature extractor (CNN-FE) has been successfully applied in a wide range of applications. Zou et al. applied CNNs to analyze targets with multiple features for image classification tasks [11]. Meanwhile, Wang et al. proposed a one-shot learning method based on CNN [12]. However, their experimental evaluating showed that CNN held a large number of parameters which considerably increased the system runtime and production costs as well as limited its applications on resource-limited platforms [12].

## 1.2 The Proposed Mango Fruit Grading Method

To improve the accuracy and real-time performance of mango fruit gradation the multi-feature grading method MFG is proposed. Considering the abovementioned limitations of the previous studies, the proposed method tackles multi-feature engineering problems, which are the most time-consuming processes in image classification, ensuring fast, accurate, and cost-effective automated grading.

We divide the vision learning algorithm into two parts. The first part is the image pre-processing, which can accurately extract and quantize mango features in the image. Due to the reasonable amount of computation, it can adapt to the real-time requirements. The second part is the machine learning classification, that combines the Random Forests theory in the application to solve the multi-feature grading problems. Finally, we build our learning model and evaluate it by experiments and two previous works: the geometry-based mass grading proposed by Momin et al. [2] and the fuzzy inference system developed by Naik et al. [4].

The key research problems of this work can be itemized as follows:

(1) Extract the values of size, surface defects, and ripeness as decisive indicators of fruit gradation for a given data set.

(2) Develop a multi-feature classification model based on the Random Forests theory.

(3) Validate the performance of the MFG method and compare it with those of other related methods from recent proposals.

The contribution of this work is as follows:

(1) A novel edge detection algorithm CFR is designed to solve the weak-edge problems in mango outline detection.

(2) To characterize the surface defects the healthy and defective parts of mangoes are resolved using local binarization techniques.

(3) Ripeness is analyzed and calibrated using the RGB color model.

(4) The Random Forests learning model predicts mango gradation for a given data set.

(5) The proposed MFG method provides a strong mango fruit gradation in terms of accuracy and real-time.

The rest of this paper is organized as follows. Section 2 demonstrates the general design of the automated mango gradation system. In section 3, a series of image processing approaches for multi-feature extraction is shown. Section 4 introduces the process of the multi-feature classification method based on the Random Forests theory. Section 5 discusses the experimental results. Finally, Section 6 is a conclusion of this work.

## 2 General Design

The automated mango gradation system mainly consists of fruit handling and vision processing units, as shown in Fig. 1. The fruits are delivered through the cleaning unit (Cleaner), single separation unit (Singularator), vision inspection unit (Inspector), and graded transmission unit (Classifier), sequentially.

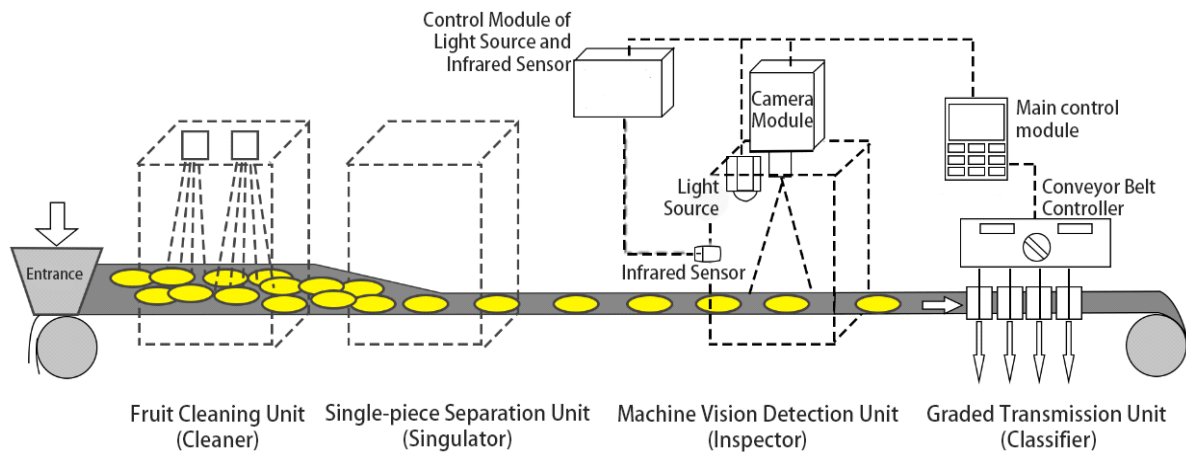


**Fig. 1.** General structure of the system

As the core of this system, image preprocessing, feature extraction, and smart classification take place in the vision inspection unit, as shown in Fig. 2. Important features are extracted from a raw feature set to construct a new feature subset. Thereafter, a machine learning model is built and trained using the multiple feature characteristics of the captured images, and then the testing dataset is fed into the model to fetch the final grading results.

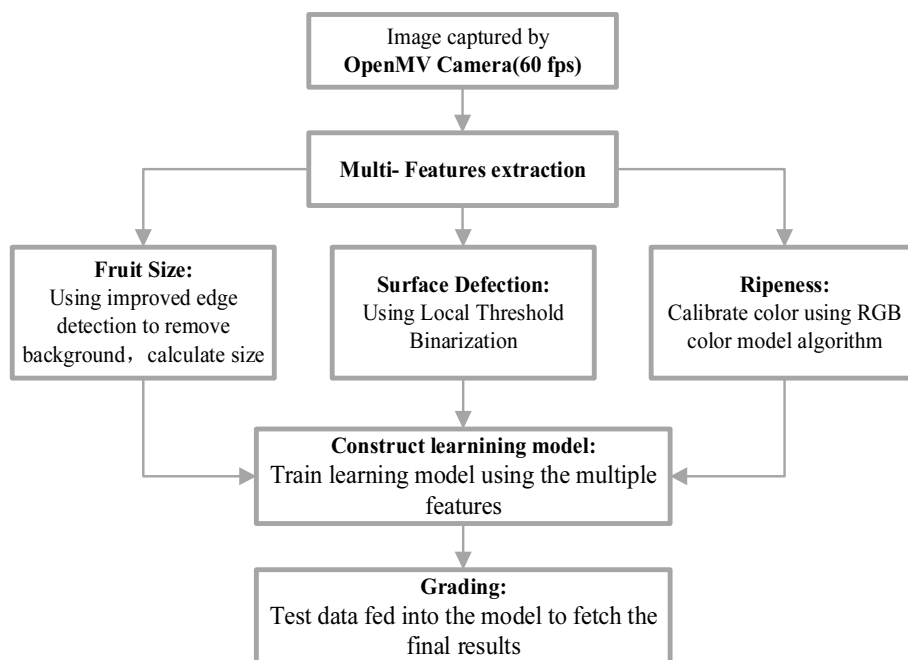


**Fig. 2.** Vision inspection unit: workflow steps

### 3 Feature Extraction

Feature selection is a necessary step before image preprocessing and machine learning. The main purpose of feature selection is to eliminate the information unrelated to the target value and to retain the key surface features of the mangoes. According to the international standards for post-harvest mango assessment [13-14], three features (size, surface defects, and ripeness) are decisive indicators of the quality of the mango fruit.

In Section 3.1, the curve-fitting route (CFR) approach of edge detection for size measurement is proposed. In Section 3.2, adaptive local-thresholding binarization to identify surface defects is presented. In Section 3.3, the RGB color model employed for analysis of the mangoes' ripeness is presented.

#### 3.1 Size Calculation

Considering that the distance between neighboring mangoes on a moving conveyor belt differs, the vision detection unit needs to determine whether the captured image contains the complete fruit contour. In this case, infrared sensors were used at the entrance of the unit to locate mangoes and trigger the photo taking. Pixels within a continuous edge form the target region, and the background outside that region is eliminated by a matrix subtraction operation.

The Canny edge detection algorithm [15] is one of the most commonly used edge detection algorithms. This algorithm uses the Gaussian filter that is able to reduce high-frequency noise in images as well as smooth edges. A typical result of Canny edge detection is consisting of discontinuous segments and multi-pixel wide edges [16], as shown in Fig. 3(b).

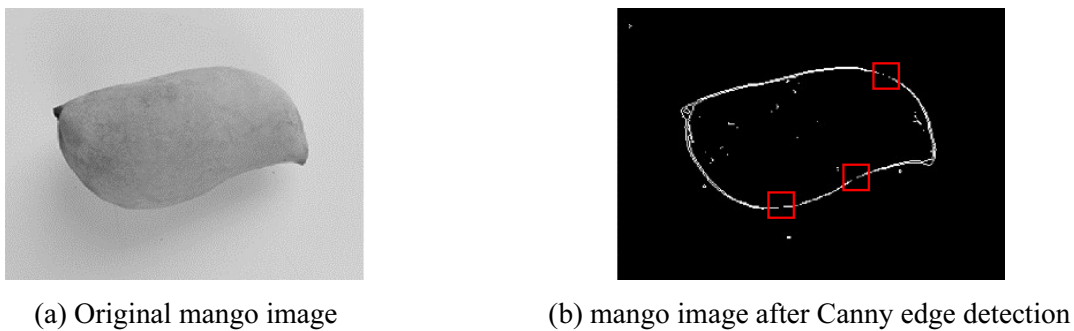


**Fig. 3.**

An adaptive edge detection method is asked to connect the pixels to reveal the vague edge segments. This method first computes a set of pixels which are assumed to be gradient peaks in an image, and then uses an efficient method called the curve-fitting route (CFR) to join these peaks. The main steps of the route are given as follows.

Step 1: First, gray level transformation is used for image enhancement, and Gaussian filtering is applied to filter out image noise. Equation (1) is a Gaussian kernel with k size = (5,5).

$$K = \frac{1}{159} \begin{bmatrix} 2 & 4 & 5 & 4 & 2 \\ 4 & 9 & 12 & 9 & 4 \\ 5 & 12 & 15 & 12 & 5 \\ 4 & 9 & 12 & 9 & 4 \\ 2 & 4 & 5 & 4 & 2 \end{bmatrix} \quad (1)$$

Step 2: The gradient intensity and direction of each pixel are calculated using the Sobel operators [12]. Equations (2) and (3) are the Sobel operators in the X and Y directions, which are used to detect edges in horizontal and vertical directions, respectively.

$$S_x = \begin{bmatrix} -1 & 0 & 1 \\ -2 & 0 & 2 \\ -1 & 0 & 1 \end{bmatrix} \quad (2)$$

$$S_y = \begin{bmatrix} -1 & -2 & -1 \\ 0 & 0 & 0 \\ 1 & 2 & 1 \end{bmatrix} \quad (3)$$

Equations (4) and (5) are the gradient intensity and direction of pixels processed by Sobel operators, respectively. The pixels with an intensity less than TH are suppressed while the others are retained, as shown in Equation (6).

$$|M| = \sqrt{M_x^2} + \sqrt{M_y^2} \quad (4)$$

$$\theta = \tan^{-1} \left( \frac{M_x}{M_y} \right) \quad (5)$$

$$g_x = \begin{cases} g_x, & \text{if } |M| > T_H \\ 0, & \text{otherwise} \end{cases} \quad (6)$$

Here, TH represents the suppression threshold, which is set according to experimental experience; and  $g_x$  represents the gray value of each pixel.

Step 3: The retained part of the image is divided into  $n \times n$  subdomains and pixels, with the largest gradient values in each subdomain marked as the “peaks.”

Step 4: The peaks are assembled to form continuous line segments by an eight-direction curve-fitting method. Fig. 4 shows the eight directions defined in the curve-fitting route.

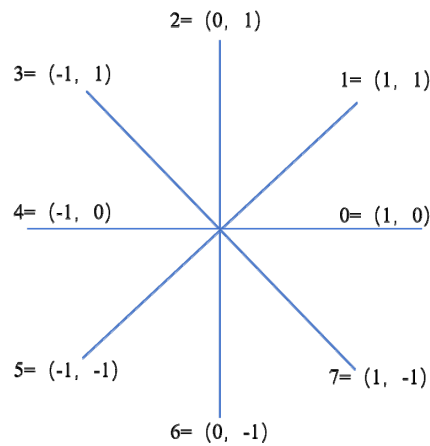


**Fig. 4.** Eight directions of the curve-fitting method

Fig. 5 illustrates how the edge is drawn using the CFR. The pixels marked in red are the “peaks” calculated using Step 3. For example, the route starts from a peak and finds the next peak in the eight-direction route. Assuming that the fitting route starts from the pixel point (15, 5), the gradient direction of the point is horizontal and to the left (Direction 4); the algorithm finds the point with the highest gradient value in Direction 4 and neighboring Directions 3 and 5, i.e., the pixel point (14, 5). This step continues until it reaches the margin of the subdomain, i.e., the pixel point (1, 9). Fig. 6 shows the difference between the conventional Canny algorithm and the CFR algorithm. After the eight-direction routing, all peaks are joined together to form a continuous one-pixel wide edge. Finally, the fruit size is calculated based on the total number of pixels  $n_s$  within the closed region.

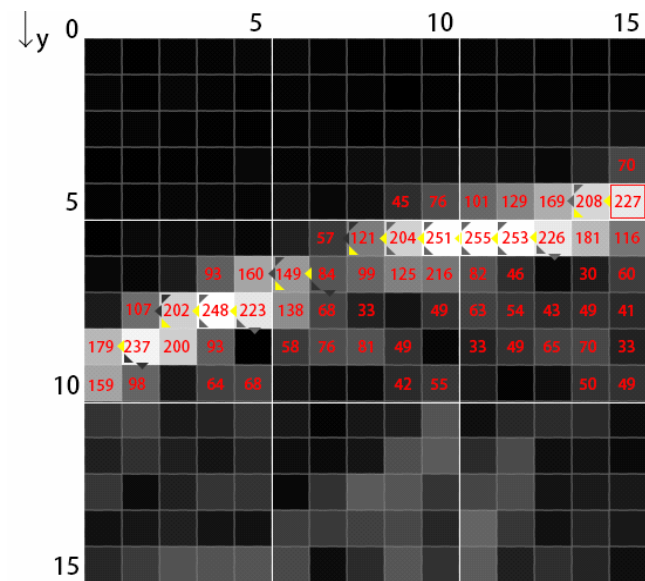


Fig. 5. Execution path of the CFR



Fig. 6. Comparison of the Canny algorithm and the eight-direction algorithm

### 3.2 Surface Defects Inspection

To inspect the surface defects of mangoes, the healthy and defective parts of mangoes are separated using image binarization techniques, and the defective pixels are counted by using the binarization results.

Considering that a sorting pipeline system is subject to factors such as poor illumination, low image quality or other factors, binarization by global thresholding may not be an effective step. Fig. 7 and Fig. 8 present the outputs of binarization under ideal and poor sunshine exposure conditions under the typical global thresholding, respectively. It is clearly observed in Fig. 8 that low image contrast makes it difficult to resolve foreground from background. The image appears half-dark and half-light. In this case, it is difficult to select a fixed threshold that works well for the entire image [17].

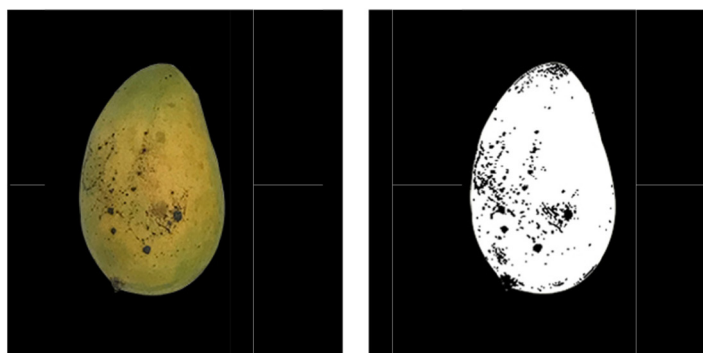
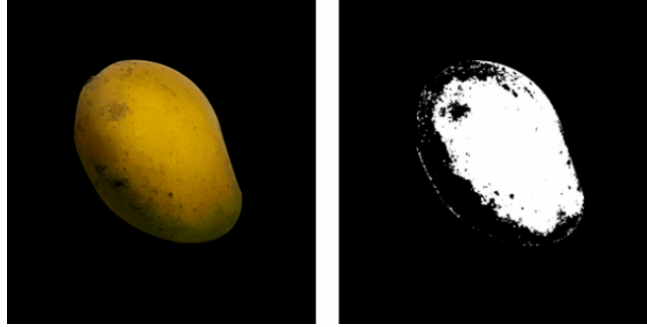


Fig. 7. Ideal sunshine exposure and binarization output



**Fig. 8.** Poor sunshine exposure and binarization output

To solve this problem an adaptive local thresholding is adopted as it changes the threshold dynamically over the image. Therefore, higher mean values are obtained in bright neighborhoods, and lower mean values are obtained in dark neighborhoods. To obtain the local thresholds, the mean value of the pixels of  $n \times n$  neighborhoods is computed as follows:

$$m(i, j) = \frac{\sum_{i=1}^n \sum_{j=1}^n p(i, j)}{n \times n}, \quad (7)$$

where  $p(i, j)$  is the gray-level of the centered pixel  $(i, j)$ , and  $n$  is the size of the neighborhood. The local threshold is expressed as in Equation (8).

$$T(i, j) = m(i, j) \quad (8)$$

Fig. 9 shows the outputs of image binarization when the neighborhood size is [6: 8]. The smaller the size of the neighborhood, the larger the amount of computation and the longer the program runtime. In this case size 7 is assumed to be the most hardware-friendly option in the experiments.

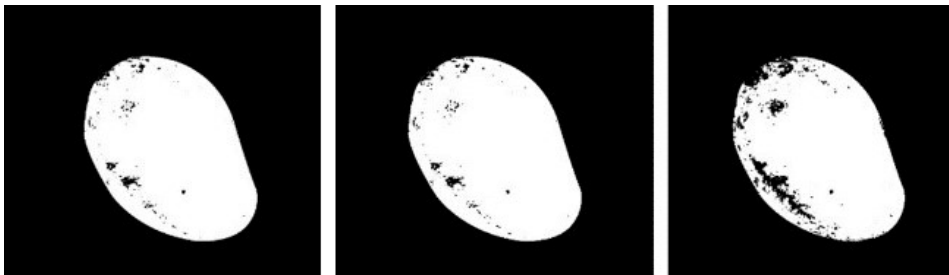


**Fig. 9.** Outputs of binarization when the neighborhood size is [6: 8]

Some noise is still observed after thresholding due to the the presence and type of surface defects. The situation can be improved if the employed threshold is not the mean value but is instead adjusted by hyperparameter  $C$ , which is a constant (Equation (9)). Fig. 10 shows that Equation (9) improves defect recognition in comparison to Equation (8).

$$T(i, j) = m(i, j) - C \quad (9)$$



**Fig. 10.** Binarization adjusted by  $C$  (size=7)

After image binarization, the pixels located within the closed region were converted into a Boolean matrix after that the percentage of defective parts can be computed using Equation (10).

$$P_d = n_d / n_s \tag{10}$$

Here,  $P_d$  represents the ratio of the defective part on the surface, and  $n_d$  represent the number of pixels in this defective part. When  $0.15 < P_d < 0.25$ , the fruit is classified as half-defective; when  $P_d > 0.25$ , the fruit is classified as defective and will not be sent for subsequent processing.

### 3.3 Ripeness Identification

Mango is a highly perishable fruit; therefore, during post-harvest processing, the partially ripe state is considered as the best state of mangoes. Ripeness is closely related to surface color, which can be expressed using the RGB color space model [18], as given by

$$A_s(R, G, B) = \frac{1}{lw} \sum_{i=1}^l \sum_{j=1}^w I_s, \tag{11}$$

where  $I_s$  represents the preprocessed RGB image, and  $l$  and  $w$  represent the length and width of an image slice, respectively. In the RGB model, the color transition from green to yellow affects the R value significantly. The mean value of R in the yellow–green junction is considered to be approximately 170 in the RGB color space [17], and the ripeness of a mango can be realized by means of simple thresholding. Fig. 11 and Fig. 12 show the histograms of the R values for different levels of ripeness. Experimentally, the ratio of  $R > 170$  pixels of a typical unripe mango is approximately 23%, whereas that of a typical mature mango is 80%.

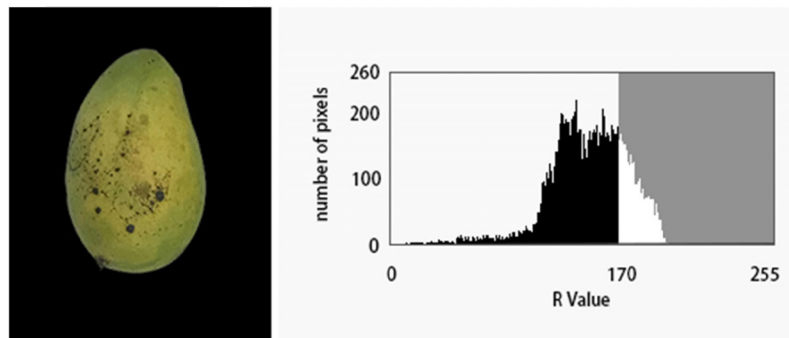


Fig. 11. R histogram of an unripe mango

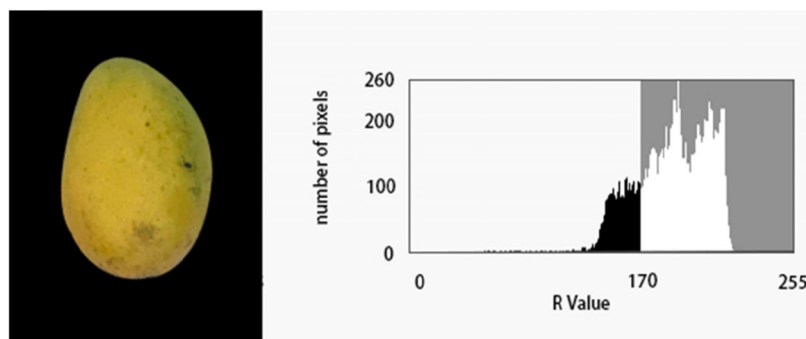


Fig. 12. R histogram of a ripe mango

## 4 Multi-feature Classifier

Size, surface defects, and ripeness of mangoes are important factors that help determine fruit gradation. However, there are conflicts among these features. For example, some mangoes are large but unripe or



show significant fruit surface defects. Therefore, it is difficult to make an accurate judgment by simple thresholding.

In this work, a multi-feature classification method (MFG) based on the Random Forests theory [19-20] is developed. It repeatedly extracts  $k$  samples from the original training sample set  $S$  to generate a training set and then generates  $k$  decision trees to form a Random Forests based on the self-selected sampling set. The classification outputs of the final result are based on the scores voted for by all classification trees. Fig. 13 describes the main idea of the Random Forests classification. The expected values of the sample dataset are expressed in Equation (12).

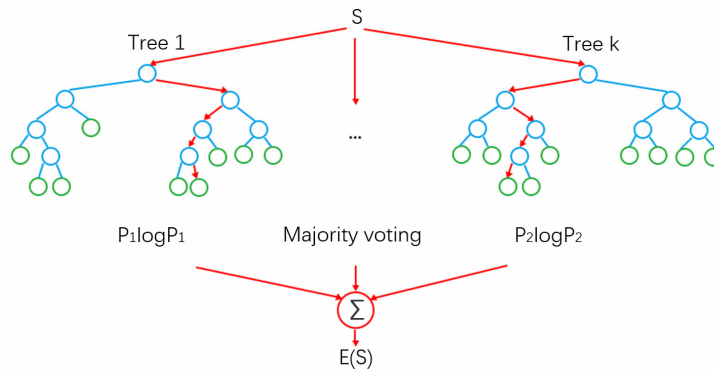


Fig. 13. Decision tree of Random Forests classification

$$E(S) = \sum_{i=1}^m P_i \log P_i (i = 1, 2, \dots, m) \quad (i = 1, 2, \dots, m) \tag{12}$$

Here,  $S$  is the dataset,  $m$  is the number of features of  $S$ ,  $P_i \cong |s_i|/|S|$ ,  $C_i$  is a classification label,  $P_i$  is the probability that any sample belongs to  $C_i$ , and  $s_i$  is the number of samples on label  $C_i$ .

The results of the Random Forests classifier depend on two important user-defined parameters: the number of decision trees ( $k$ ), and the number of feature labels ( $m$ ). To determine the best parameters for the classifier, the number of Random Forests decision trees is set to [20, 40, 60, 80, 100, 120, 140, 160], and the three feature labels are “total pixels of fruit,” “defect pixels,” “pixels with  $R > 170$ .”

Then, 300 mango samples were used in the Random Forests classifier, including varieties of Tai Nong mango (TN), Golek (GL), Gui Fei mango (GF), and Jin Huang mango (JH) — mainly from Taiwan, Guangdong, and Hainan. The classification algorithm divides the sample dataset into training (70% of the total) and testing datasets (30% of the total). Table 1 shows part of the training dataset. Table 2 shows the prediction accuracy of the training model under different  $k$  values in the range of 20-160. When the number of decision trees is 100, the training model achieves a stable prediction accuracy and stable real-time performance.

Table 1. Part of Training dataset

No.	Varieties	Number of			Ripeness	Grade
		Total pixels	Defect pixels	R>170 pixels		
1	TN	36219	42	35523	89	1
2	TN	19603	87	16953	78	1
3	GF	39038	1072	18057	45	3
4	JH	58401	831	45304	76	2
5	JH	52082	307	46009	83	1
6	GL	33002	51	15940	91	1
7	TN	17011	68	14012	82	1
8	GF	37305	270	28057	87	1
9	GF	38706	638	21705	69	2
10	JH	56850	2318	26092	34	3

**Table 2.** Prediction accuracy of the training model (k values)

No.	k	Runtime (ms)	Accuracy
1	20	82	0.844
2	40	93	0.878
3	60	116	0.894
4	80	121	0.926
5	100	130	0.944
6	120	145	0.946
7	140	166	0.949
8	160	189	0.950

## 5 Experiment and Comparison

The performance of the MFG method developed in this work is validated by the testing dataset. Throughout the experiments, the accuracy and real-time performance of the proposed method are compared with those of two other algorithms from recent proposals.

### 5.1 Experimental Environment

An OpenMV camera is employed in the image-capture unit, with an embedded photosensitive OV7725 sensor, and 320×240 8-bit RGB three-channel images under 60 fps. The shooting distance of the camera module is set to 30 cm.

### 5.2 Test Results

The MFG algorithm is tested on 90 test samples. Using the existing pre-trained model, the testing dataset can be transformed into target values (grade of mangoes). To evaluate the performance on the test set, the main features were manually observed and measured. Table 3 shows some size measurement results obtained from program runs and manual measurements. It is observed that the MFG method that includes the proposed CFR edge detection generates highly accurate measurements since the accuracy of the size calculation received is nearly 98.4%. Meanwhile, the average value of ripeness accuracy is 96.6% if human expert grading is assumed to be 100% accurate.

**Table 3.** Some results of size measurements

Variety	Total number of pixels	Calculated area (cm <sup>2</sup> )	Actual area (cm <sup>2</sup> )	Number of defect pixels	Defect ratio	Size error (%)
GL	34601	178.5	179.9	41	0.12	0.76
TN	18930	97.7	98.4	603	3.19	0.73
GF	40012	206.5	210.5	377	0.94	1.62
JH	57538	296.9	299.2	410	0.71	0.77
JH	52082	268.7	272.1	307	0.59	1.23
GL	33002	170.3	171.5	51	0.15	0.71
TN	17011	87.8	88.2	68	0.40	0.48
GF	37305	192.5	194.8	270	0.72	1.18
GF	38706	199.7	202.4	638	1.65	1.32
JH	56850	293.3	297.9	2318	4.08	1.53
GL	34601	178.5	179.9	41	0.12	0.76
TN	18930	97.7	98.4	603	3.19	0.73
GF	40012	206.5	210.5	377	0.94	1.62
JH	57538	296.9	299.2	410	0.71	0.77

The results of the testing gradation are shown in Table 4. Accuracy in a three-class classification can be calculated from Equation (13).

$$\text{Accuracy} = \frac{\sum_{i=1}^m \frac{TP_i + TN_i}{TP_i + TN_i + FP_i + FN_i}}{N} \quad (m = 1, 2, 3) \quad (13)$$

Here,  $TP_i$ ,  $TN_i$ ,  $FP_i$ , and  $FN_i$  are the number of true positives, false positives, true negatives, and false negatives in each grade, respectively. Compared to Grades 1 and 2, the grading error is slightly higher in Grade 3, especially when the target training data are considerably noisy due to the surface characteristics of the Grade-3 mango. Moreover, the statistics given in Table 4 indicate that 94.4% of the total testing samples are graded correctly.

**Table 4.** Grade testing results

Input grade	Quantity	Recognized as grade		
		1	2	3
1	38	36 (TP)	2 (FP)	0 (FN)
2	36	1 (FP)	33 (TP)	2 (FP)
3	16	0 (FN)	0 (FN)	16 (TP)
Total	90	37	35	18
Accuracy (%)	94.4	97.3	94.3	88.9

### 5.3 Comparison

Two mango grading methods are compared with the MFG method proposed in this work. The first one is the geometry-based mass grading proposed by Momin et al. in 2017 [2]. The other one is the fuzzy inference system developed by Naik et al. in 2017 [4]. Both methods were recently utilized to study features and train learning models. Table 5 presents the results of our comparison where the two methods are referred to as methods GBG and FIS.

The summary of the performance comparison results indicates the following:

(1) The number of quality factors that are used in the design critically influences the performance of grading systems. The GBG is addressing the quality grading of mangoes based on two factors: shapes and sizes. The time consumed for a sample is 140ms. The grading accuracy, meanwhile, is less than 80% due to the small number of fruit features used in the method.

(2) In the FIS design, a fuzzy inference system based on the training phase and fuzzy rules is used for the decision-making process. The testing accuracy is nearly 90% and the time needed to grade a mango is more than 2 seconds which is time consuming for grading.

(3) The MFG that employed the Random Forests classifier generates statistically better mango gradation results. Using the optimal solution of the number of decision trees, the grading accuracy and processing time for a single mango is reasonable.

**Table 5.** Testing results of different methods

	GBG	FIS	MFG
Size accuracy (%)	97.0	96.0	98.4
Ripeness accuracy (%)	--	86	96.6
Grading accuracy (%)	79.0	89.0	94.4
Runtime/fruit (ms)	140	2300	145

## 6 Conclusions and Future Work

To improve the accuracy of mango fruit gradation, an intelligent multi-feature grading method MFG is proposed. The machine learning method consists of image preprocessing and learning classification.

(1) In the image preprocess the MFG extracts sizes, surface defects, and ripeness as decisive indicators of fruit gradation for a given data set. An edge detection algorithm based on the proposed CFR approach is designed to solve the “weak-edge” problems that frequently occur in the conventional edge algorithms. The key achievement of using the CFR is to join gradient peaks to form a set of one-pixel wide edge segments. Experimental results show that the edge segments drew by the CFR is clearer and more

coherent as well provide important basis for accurate size measurements.

(2) A learning model is developed based on Random Forests theory, which is used to improve the multi-feature classification ability. The “train–predict” model provides a stronger prediction in terms of accuracy and speed compared to other state-of-the-art methods from recent proposals.

In this paper, the study is mainly focused on the external quality features of mangoes: size, color and surface defects. For the future work, we will explore internal quality features of mangoes, such as smell, nutritive value, firmness; and we prefer nondestructive approaches to quantize all these internal quality features and analyze their influences on the fruit grading.

## Acknowledgments

This work is supported by the following projects:

(1) 2017 Guangdong Special Innovative Education and Scientific Research Fund (Project Number: 2017GGXJK073).

(2) 2019 Zhongshan Social Public Welfare Science and Technology Research Project (Project Number: 2019B2082).

## References

- [1] Worldatlas, The top mango producing countries in the world. < <http://worldatlas.com/articles/the-top-mango-producing-countries-in-the-world.html>> 2018 (accessed 18.09.04).
- [2] M.A.Momin, M.T. Rahman, M.S. Sultana, Geometry-based mass grading of mango fruits using image processing, *Information Processing in Agriculture* 4(2)(2017) 150-160.
- [3] C.S. Nandi, B. Tudu, C. Koley, Computer vision based mango fruit grading system, in: *Proc. 2014 International Conference on Innovative Engineering Technologies*, 2014.
- [4] N. Sapan, P. Bankim, Thermal imaging with fuzzy classifier for maturity and size based non-destructive mango, in: *Proc. 2017 International Conference on Emerging Trends and Innovation*, 2017.
- [5] Y.A. Ohali, Computer vision based date fruit grading system: design and implementation, *Journal of King Saud University - Computer and Information Sciences* 23(1)(2011) 29-36.
- [6] I. Yung, Y. Maccarana, G. Maroni, F. Previdi, Partially structured robotic picking for automation of tomato transplantation, in: *Proc. 2019 IEEE International Conference on Mechatronics*, 2019.
- [7] M.P. Arakeri, Lakshmana, Computer vision based fruit grading system for quality evaluation of tomato in agriculture industry, in: *Proc. 7th International Conference on Communication, Computing and Virtualization (2016)* 2016.
- [8] N. Innocent, Tomato volume and mass estimation using computer vision and machine learning algorithms: cherry tomato model, *Journal of Food Engineering* 263(2019) 288-298.
- [9] F. Longsheng, A novel image processing algorithm to separate linearly clustered kiwifruits, *Biosystems Engineering* 183(2019) 184-195.
- [10] W. Wang, Y. Fang, J. Liu, Z. Wang, Blueberries grading detection algorithm based on machine vision, *Modern Electronics Technique* 41(13)(2018) 38-42.
- [11] Y.-X. Zou, J.S. Yu, Z.-H. Chen, J. Chen, Y. Wang, Convolutional neural networks model compression based on feature selection for image classification, *Control Theory and Applications* 34(6)(2017) 746-752.
- [12] K. Wang, W. Chen, C. Liu, D. Liu, H. Han, One-shot learning method based on convolutional neural network for intelligent robot, *Journal of Computers* 30(230)(2)(2019) 165-172.

- [13] R. Holmes, P. Hofman, L. Barker, Mango Quality Assessment Manual: A Guide to Assessing the Post-harvest Quality of Australian Mangoes, The State of Queensland, Department of Employment, Economic Development and Innovation, 2009.
- [14] United States Standards for Grades of Mangoes, United States Department of Agriculture, 2007.
- [15] J. Canny, A computational approach to edge detection, IEEE Transactions on Pattern Analysis and Machine Intelligence, 8(6)(1986) 679-698.
- [16] C. Akinlar, E. Chome, CannySR: using smart routing of edge drawing to convert Canny binary edge maps to edge segments, in: Proc. 2015 International Symposium on Innovations in Intelligent SysTems and Applications (INISTA), 2015.
- [17] M. Seul, L. O’Gorman, M J. Sammon, Practical Algorithms for Image Analysis with CD-ROM: Description, Examples, and Code, Cambridge University Press, 2000 (Chapter 3).
- [18] D. Pascale, A Review of RGB Color Spaces, BabelColor, Montreal, 2003.
- [19] T.K. Ho, Random decision forests, in: Proc. the 3rd International Conference on Document Analysis and Recognition, 1995.
- [20] J.L. Speiser, M.E. Miller, J.A. Tooze, E.H.-S. Ip, A comparison of random forests variable selection methods for classification prediction modeling, Expert Systems with Applications 134(2019) 93-101.